ZnO Nanomulberry and Its Significant Nonenzymatic Signal Enhancement for Protein Microarray

Yingshuai Liu,[†,‡,§] Weihua Hu,[†,‡,§] Zhisong Lu,[†,‡,§] and Chang Ming Li*[,†,‡,§]

[†]Institute for Clean Energy and Advanced Materials, Southwest University, No. 2 Tiansheng Road, Chongqing 400715, China
[‡]Faculty of Materials and Energy, Southwest University, No. 2 Tiansheng Road, Chongqing 400715, China
[§]Chongqing Key Laboratory for Advanced Materials and Technologies of Clean Energies, Chongqing 400715, China

ABSTRACT: It is very challenging to make a highly sensitive protein microarray because of its lack of a universal signal amplification method like PCR used in DNA microarray. The current strategies to improve the sensitivity mainly rely on a unique nanostructured substrate or enzymatically catalyzed signal amplification, of which the former requires a complicated and time-consuming fabrication process while the latter suffers from high cost and poor stability of enzymes as well as downstream biochemical reactions. In this work, an inexpensive ZnO nanomulberry (NMB) decorated glass slide is investigated as a superior substrate to nonenzymatically amplify the signal of protein microarray for sensitive detection, accomplishing a limit of detection (LOD) of 1 pg mL^{-1} and a broad dynamic range of 1 pg mL^{-1} to 1 μg mL^{-1} to detect an important cancer biomarker, carcinoembryonic antigen (CEA) in 10% human serum. The excellent performance is attributed to ZnO NMB possessing high-density loading of capture antibody and intrinsic enhancement of fluorescence emission. The substrate preparation is simple without using any expensive equipment and complicated technique while offering advantages of low autofluorescence, versatility for various fluorophores, and excellent compatibility with existing microarray fabrication techniques. Thus, a ZnO NMB based protein microarray holds great promise for developing a low cost, sensitive, and high throughput protein assay platform for broad applications in both fundamental research and clinical diagnosis.

KEYWORDS: ZnO nanomulberry, fluorescence amplification, protein microarray, immunoassay, biomarker detection

SEM image of ZnO nanomulberrys (NMBs)

Immunoassay on ZnO NMB-coated slide

ZnO NMB-enabled fluorescence enhancement
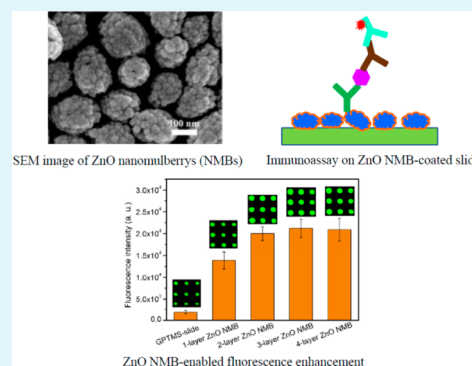
1. INTRODUCTION

In the postgenome era, protein microarray has emerged as a powerful tool for proteomic studies owing to its merits such as high-throughput, fast assay, and small volume sample consumption.[1,2] Although protein microarrays have been widely used in various areas including fundamental bioscience, disease diagnostics, and drug discovery,[3−7] it still remains a big challenge to achieve high sensitivity because of the lack of a universal signal amplification method like PCR used in DNA microarray. Currently, enzymatically catalyzed signal amplification[8−10] is the most popular approach to improve the performance of protein microarray. Unfortunately, it requires expensive and unstable enzyme as well as additional biochemical reactions, severely limiting their practical applications.

Fluorescence is a prevailing readout technique used in biomolecular detection, particularly on microarray platform.[11,12] Nanostructured substrate-assisted fluorescent enhancement is an alternative scheme to improve sensitivity of fluorescence-based protein assays without use of enzyme. A number of nanomaterials with specific patterns or structures have been reported as substrates for fluorescence enhancement.[13−19] Plasmonic film made from noble metals is the most popular substrate, but the high cost and complicated fabrication processes restrict their applications. It is also still very

challenging to fabricate a uniform metal structure on a microscope slide for microarray application. In addition, since the plasmonic enhancement depends on the overlap between plasmon resonance of nanostructured materials and excitation/emission wavelength of fluorophores,[13] only those with specific spectral characteristics can be amplified. Metal mirror[20] and photonic crystal[15] assisted fluorescence enhancements are successfully developed to improve the performance of immunoassays. However, multiple manufacturing steps and expensive equipment are needed to fabricate these specific surfaces or structures.

ZnO nanorod has been used to amplify fluorescence signal for detection of DNA and proteins,[12,21,22] but all these studies are performed on prepatterned ZnO nanorod arrays, which requires expensive microfabrication techniques and is difficult for large-scale manufacturing, thus limiting its applications. Recently, random oriented ZnO nanorods have been prepared on a microscope glass slide as a microarray substrate with fluorescence-enhancing capacity, which does not need the patterning processes.[23] However, the hydrothermally grown ZnO nanorods commonly emit yellow-green fluorescence

centered at ~580 nm,[24] which is similar to the emission of a popular microarray scanner, resulting in strong background and low signal-to-noise ratio. Thus, a substrate with intrinsic fluorescnece-enhancing capability and low autofluorescnece is greatly desired to improve signal-to-noise ratio and sensitivity of protein microarrays.

In this work, ZnO nanomulberry (NMB) with very low autofluorescence is explored as a superior fluorescence-enhancing material for sensitive and high-throughput protein microarray. The ZnO NMBs were synthesized with a facile solution-phase route in diethylene glycol (DEG) and coated homogeneously on glass slides by a simple drop-coating process without need of any expensive equipment and complicated processes. Highly sensitive microarray immunoassays are demonstrated by detection of an important cancer biomarker, carcinoembryonic antigen (CEA) as a model target on ZnO NMBs-coated glass slide. The high performance is attributed to the excellent fluorescence-enhancing capability, negligible autofluorescence, and large specific surface area of ZnO NMBs. The ZnO NMB based protein microarray holds great promise for developing a low cost, sensitive, and high throughput protein assay platform for various applications.

2. EXPERIMENTAL SECTION

2.1. Chemicals and Reagents. Plain microscope glass slides with dimension of 75 mm × 25 mm × 1 mm are purchased from Fisher Scientific. Zinc acetate dihydrate ($Zn(OAc)_2 \cdot 2H_2O$, ≥98%), diethylene glycol (DEG, ≥99.0%), (3-glycidoxypropyl)trimethoxysilane (GPTMS, 98%), glycerol, Triton X-100, 0.01 M phosphate buffered saline (PBS, pH 7.4), Cy3-labeled goat anti-rabbit IgG, and peroxidase-conjugated rabbit anti-goat IgG are received from Sigma-Aldrich. Cy3-tagged goat anti-human IgG is ordered from Invitrogen. Monoclonal mouse anti-CEA, polyclonal rabbit anti-CEA, and CEA were purchased from Fitzgerald.

2.2. Synthesis and Characterization of ZnO NMBs. ZnO NMBs are prepared by a modified polyol-mediated solution-phase hydrolysis described previously.[25] Specifically, 1.1 g of $Zn(OAc)_2 \cdot 2H_2O$ is completely dissolved in 50 mL of DEG with the assistance of ultrasonication to obtain $Zn(OAc)_2$/DEG stock solution. The freshly prepared stock solution is placed into a 100 mL conical flask, which is then immersed in preheated silicon oil (180 °C) for 5 min under magnetic stirring at 300 rpm. Subsequently, 0.5 mL of deionized (DI) water is rapidly injected into the hot mixture to initiate the hydrolysis of $Zn(OAc)_2$. The mixture is kept at 180 °C for 10 min under continuous stirring to form a slightly turbid solution. After removal of the heat source, the solution is cooled to room temperature (rt) under continuous stirring. The product is diluted with an equal volume of ethanol, followed by centrifugation at 5000 rpm. The precipitate is washed three times with ethanol by repeating the centrifugation process and finally dispersed in pure ethanol for further use.

The size and morphology of the as-prepared NMBs are characterized by field effect scanning electron microscopy (FE-SEM, JEM-6700F) and transmission electron microscopy (TEM, JEM-2100). The XRD pattern is recorded by a D8 advance X-ray diffractometer (Bruker AXS, German) with Cu Kα radiation (λ = 0.154 18 nm).

2.3. Preparation and Silanization of ZnO Coated Slides. Plain glass slides are ultrasonically cleaned by ethanol for 10 min and then dipped in 3 M KOH for 1 h at rt to introduce a hydroxyl group. After being intensively rinsed with DI water, the slides are dried under nitrogen flow. To prepare ZnO NMB coated slides, 60 μL of ZnO NMB solution at 4.6 mg mL^{-1} in ethanol is dropped on one end of each slide. Then the solution is slowly allowed to flow over the whole slide. After the sample is dried, the coating process is repeated to get desired coating layers. The coated slides are annealed at 150 °C for 4 h to promote the adhesion of ZnO NMB. Then ZnO-coated slides are hydroxylated by UV irradiation for 15 min in a moist atmosphere to improve silanization efficiency.[26] Silanization is then carried out in 5% (v/v) GPTMS ethanol solution for 1 h at rt. These slides are thoroughly washed with ethanol and DI water, followed by blow drying. Subsequently, the silanized slides are baked at 110 °C for 2 h in a vacuum oven.

2.4. Quantification of Protein Immobilization. Both GPTMS functionalized glass slide (GPTMS slide) and GPTMS modified ZnO NMB coated slide (GPTMS-ZnO NMB-slide) are separated by hydrophobic pen to 5 rectangle areas with dimensions 1 cm × 2 cm. Peroxidase-conjugated anti-goat IgG at 100 μg mL^{-1} prepared in printing buffer (0.01 M PBS + 2.5% glycerol + 0.003% Triton X-100) is deposited in each area manually by pipet with 3 spots per area and 1 μL per spot. The deposited slides are then incubated for 4 h at rt. After the samples are washed with 0.05 M Tris buffered saline (TBS with 0.05% Tween 20), 100 μL of enzyme substrate TMB blue (soluble) is simultaneously applied to each area with multichannel pipet, followed by incubation for 1 min under gentle shaking. Subsequently, 100 μL of 0.5 M H_2SO_4 is immediately added to each area to terminate the reaction. The yellow solutions were transferred to a 96-well microplate to measure their absorbance at 450 nm by microplate reader.

2.5. Fabrication of Protein Microarrays and Immunoassay. Protein dissolved in printing buffer is first transferred to a 384-well microplate as a printing source. Then robotic contact printing is performed by PersonalArrayer 16 (CapitalBio Corporation, China) at rt and 60% humidity. Around 0.3 nL of sample per spot is printed on substrate. The printed slides are incubated overnight at rt to allow covalent bond formation between the amine group on protein and the epoxy group on substrate. After the incubation, all slides are washed 3 times for 2 min each with TBS to completely remove unbound protein molecules. For sandwich immunoassay, the slides are passivated with 1% BSA prepared in 0.01 M PBS for 2 h at rt. Antigen (analyte), recognition antibody, and fluorophore-labeled secondary antibody are subsequently applied to each printed microarray (Scheme 1). For antibody−antigen reaction, a 1 h incubation is carried out at 37 °C for each step.

Scheme 1. Fabrication of ZnO NMB-Based Antibody Microarray (a) and the Immunoassay of CEA (b)
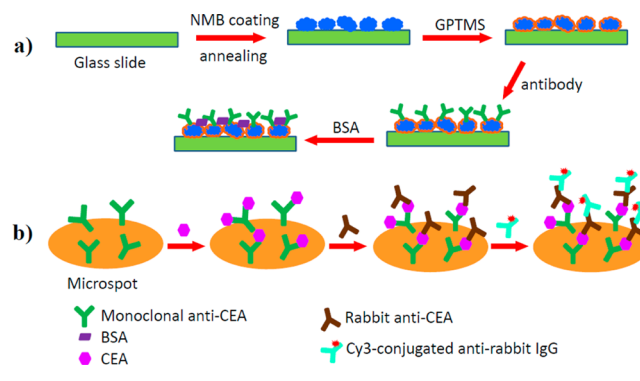
2.6. Imaging and Data Analysis. After completion of all immunoreaction steps, each slide is thoroughly rinsed with TBS and DI water and then scanned with a microarray scanner (LuxScan 10K, CapitalBio Corporation, China) under excitation of 543 nm. The acquired fluorescence images are quantitatively analyzed with LuxScan 3.0 analysis software. Local background-subtracted signal intensity of each spot is utilized for downstream statistical analysis and plot.

3. RESULTS AND DISCUSSION

3.1. Properties of As-Prepared ZnO NMB. Synthesis of spherical ZnO nanocrystal clusters has been reported but uses a complicated experimental setup[25] or/and assistance of a surfactant such as poly(acrylic acid) (PAA).[27] In this work, the ZnO NMBs are synthesized with a scalable polyol-mediated approach without use of any surfactant and complicated setup.
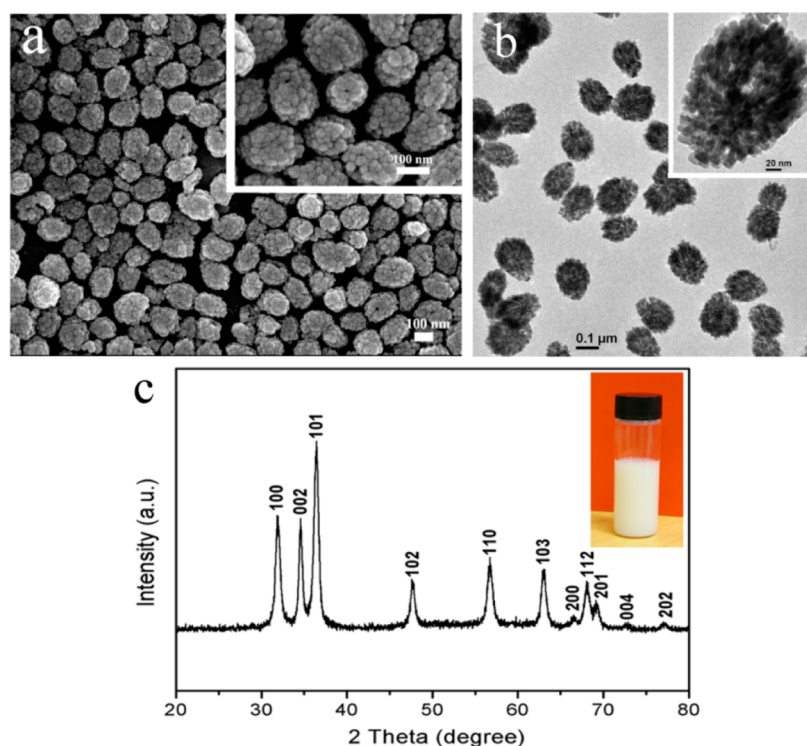
Figure 1. FE-SEM (a) and TEM (b) images of ZnO NMB with different magnifications, XRD pattern (c), and ethanol solution (c, inset) of ZnO NMB.

FE-SEM images show that the obtained product is mono-dispersed spheroidic nanoclusters with uniform size of 130 ± 20 nm in diameter (Figure 1a). Each nanocluster consists of many small primary nanocrystals with a diameter of about 10 nm (Figure 1a inset). The size and characteristics are further confirmed by TEM images as shown in Figure 1b. Since the nanocluster looks like mulberry, it is ironically called nano-mulberry (NMB). The mulberry-like cluster is produced via the well-documented two-stage growth process, in which primary nanocrystals are first formed via nucleation in supersaturated solution and then they spontaneously aggregate into larger secondary clusters.[25,27] The spheroidic shape probably results from the relatively inhomogeneous heating of hot plate equipped with silicon oil bath. Even magnetic stirring is applied continuously, and a temperature gradient may be present in bulk solution, leading to anisotropic aggregation of primary ZnO nanocrystals. The rough surface combined with a high surface-to-volume ratio of NMB provides a large specific surface area for high protein loading capacity, which is very critical for heterogeneous protein detection. XRD pattern (Figure 1c) illustrates a crystalline structure of the mulberry-like nanocluster, which can be indexed to wurtzite-type hexagonal ZnO. It is worth noting that the resulting ZnO NMBs have good dispersity in ethanol (Figure 1c, inset), which makes the homogeneous coating on glass slides very easy. Taking into account the simple preparation, large specific surface area, and good dispersibility, ZnO NMBs can be an attractive coating material for protein microarray application.

3.2. ZnO NMB Coating on Glass Slides. ZnO NMB coated glass slides were prepared according to the procedures discribed in Experimental Section. ZnO NMB distribution and surface morphology of coated slides are first characterized by FE-SEM. Figure 2a–d shows the SEM images of ZnO NMB coated slides with different coating layers. It is seen that ZnO NMBs are coated homogeneously on slides after one- and two-layer coating. Only half-monolayer of ZnO NMB is observed from one-layer coated slide (Figure 2a), while nearly a full monolayer with occasional aggregations is formed after two-layer coating. However, significant aggregations are shown for three- and four-layer-coated slides, resulting in poor homogeneity. Surface morphology of each slide is further monitored with an atomic force microscope (AFM). Three-dimensional AFM images (Figure 2a–d, insets) show that the thickness of the coating layer is enhanced with the increase of coating layer. Homogeneous and small dots featured surface is observed from one-layer coated substrate, indicating no multilayer cluster is presented. After two-layer coating, the surface is dominated by high density of small dots and a few bigger islands, demonstrating relatively good homogeneity. As for three- and four-layer-coated surface, the sparse and irregular big islands indicate the serious aggregations and poor homogeneous distributions of ZnO NMB, which is well consistent with SEM results. From combination of AFM and SEM data, a two-layer coating gives both high surface coverage and good homogeneity. Figure 2e (bottom) is the photograph of two-layer ZnO NMB-coated glass slide. A uniform milk-white layer completely covers the whole slide compared with bare slide (top). In addition, autofluorescence of substrate is one of the concerns in fluorescence based analysis. Very low autofluorescence is observed from ZnO NMBs coated slide under excitation at 543 nm, while a quite high inherent fluorescence is obtained from ZnO nanorods coated surface (Figure 2f, top). Thus, higher signal-to-noise ratio is expected on ZnO NMBs slide in comparison with ZnO nanorods slide.

3.3. Signal Enhancement and Reproducibility. To evaluate and optimize ZnO NMB-enabled signal enhancement, five groups of 3 × 3 microarrays of Cy3-conjugated goat anti-human IgG are printed on GPTMS-ZnO NMBs slides with
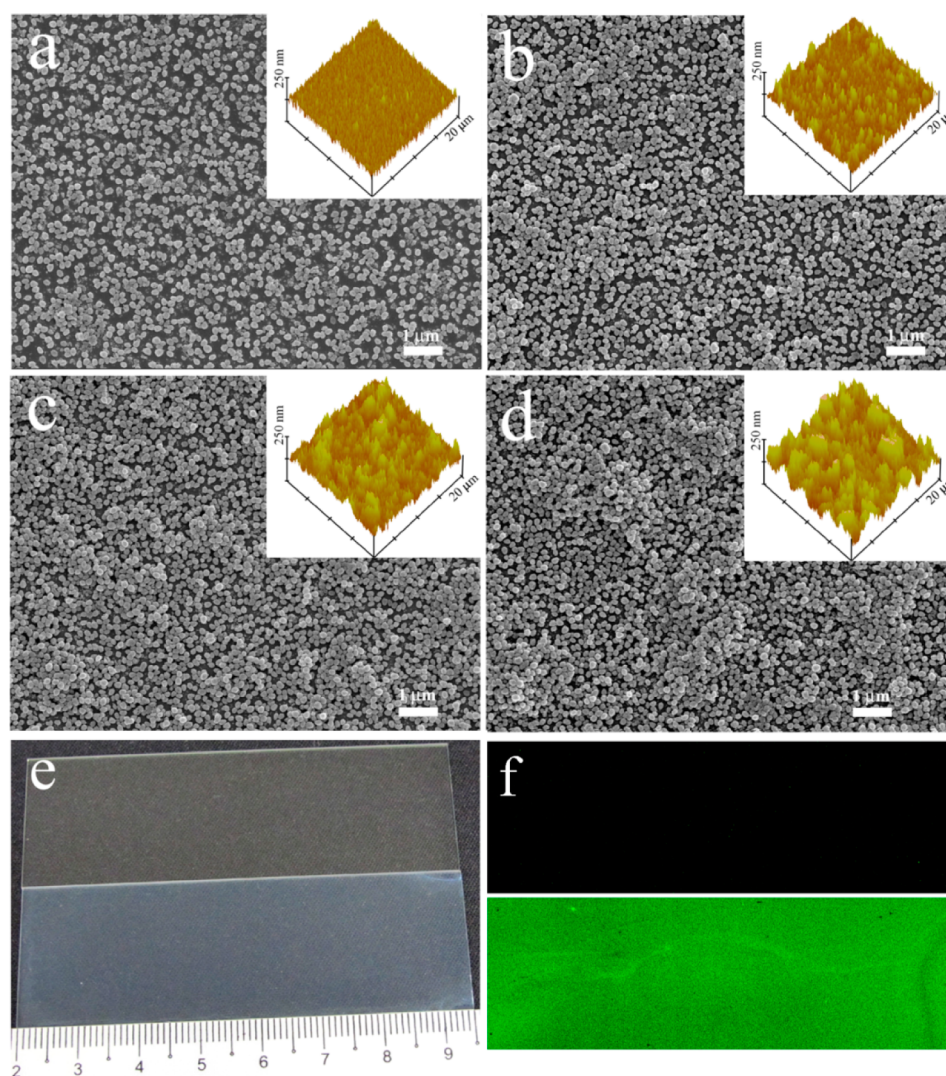
Figure 2. FE-SEM images of ZnO NMBs-coated glass slides with one-layer (a), two-layer (b), three-layer (c), four-layer (d) coatings; photographs of bare (top) and two-layer ZnO NMBs (bottom) coated slides (e); autofluorescence of ZnO NMBs coated (top) and ZnO nanorods coated (bottom) slide under 543 nm excitation (f).

different coating layers. The same microarrays are prepared on GPTMS slide for comparison. The fluorescence images and corresponding signal intensities obtained from each slide are shown in Figure 3.

It is clearly seen that significantly enhanced signal is observed from all ZnO NMBs-coated slides compared with GPTMS slide. In addition, fluorescence intensity is increased with the number of coating layers ($\leq$3), while no further signal increase is observed from substrates with more coating layers (>3). It is easily understood that the low fluorescence-enhancing effect of one-layer coated slide is attributed to the low coverage of ZnO NMB (Figure 2a). Apparently, the increase of surface coverage (for coating layers of $\leq$3) results in the improvement of signal amplification as shown in Figure 3. For four-layer coating, the severe aggregation of ZnO NMB reduces its surface utilizing efficiency for protein attachment; thus, no further signal enhancement is achieved compared to three-layer surface. Although higher signal intensity is obtained from three- and four-layer ZnO NMBs coated slide, big standard deviations are observed because of the heterogeneous distribution of ZnO NMBs as shown in Figure 2c,d. The larger deviation indicates relatively poor reproducibility and reliability of microarray.
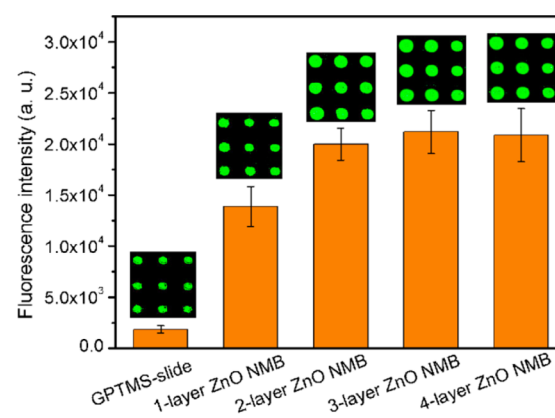
Figure 3. Fluorescence images and fluorescence intensities observed from GPTMS slide and GPTMS-ZnO NMB slide with different coating layers.

Overall, a two-layer coated substrate renders high signal intensity and good signal reproducibility. It is considered as an optimal substrate, from which the signal is enhanced by more than 1 order of magnitude in comparison to GPTMS

7731

dx.doi.org/10.1021/am501015p | *ACS Appl. Mater. Interfaces* 2014, 6, 7728−7734

slide, demonstrating significant fluorescence amplification enabled by ZnO NMB. Similar to ZnO nanorods, the enhanced fluorescence emission can be explained by changes in photonic-mode density and/or inhibition of fluorophores' self-quenching.[12] The NMB may induce modifications of radiative and nonradiative decay rate, resulting in predominantly fast radiative decay, which contributes to the enhancement of fluorescence emission. In addition, the ZnO NMBs may disable traps in energy levels and reduce self-quenching of surface-attached fluorophores.

Reproducibility of microarray substrate is very critical for quantitative protein analysis, especially in diagnosis. Coefficient of variation (CV) is calculated to evaluate the repeatability of ZnO NMBs slides.[28] The intraslide and interslide CVs are calculated at around 6% and 11%, respectively, demonstrating a very good repeatability for both intraslide and interslide (Figure 4).
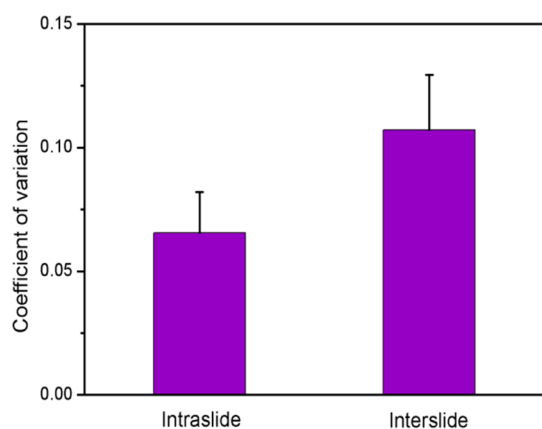

Figure 4. Intraslide and interslide CV of GPTMS-ZnO NMB slide.

3.4. Protein Immobilization Capacity.
For heterogeneous immunoassay, antibody or antigen is generally immobilized on substrate surface to capture the corresponding analytes, and then nonbound target molecules are washed away.[29,30] Theoretically, the larger the amounts of capture molecules are immobilized on surface, the more targets can be captured during assays, resulting in high detection sensitivity and broad dynamic range.[2,31] Thus, protein immobilization is very critical to improve protein microarray performance.[1,32−35] Protein immobilization on GPTMS slide and GPTMS-ZnO NMB slide is evaluated by enzyme-catalytic colorimetric assay as described in Experimental Section. The measured absorbance is proportional to the amount of immobilized peroxidase-tagged antibody. Surface density of the attached protein is determined by the spot area-normalized absorbance. Figure 5 shows that the protein loading on GPTMS-ZnO NMB slide is ~1.6 times that on GPTMS slide, which apparently results from rough surface and large surface-to-volume ratio of the ZnO NMB as discussed above, which could increase the probe loading for signal amplification. Considering more than 1 order of magnitude signal amplification is totally accomplished from a two-layer ZnO NMB slide (Figure 3), ~6 times signal enhancement should be contributed from intrinsic ZnO NMB fluorescence amplification.

3.5. Antibody Microarray for CEA Detection.
The performance of protein microarrays fabricated on GPTMS-ZnO NMB slide is examined by sandwich immunoassay in 10% human serum with CEA as model analyte. Monoclonal mouse
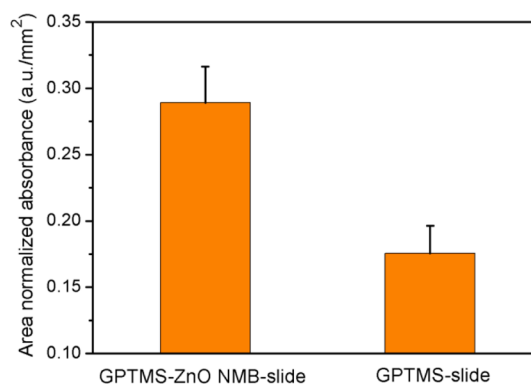

Figure 5. Quantification of protein immobilization on GPTMS-ZnO NMB slide and GPTMS slide.

anti-CEA prepared in printing buffer is printed on ZnO NMBs coated slides as capture antibody. Ten subarrays in 4 × 4 pattern are obtained on each slide. Various concentrations of CEA from 0.1 pg mL^{-1} to 10 μg mL^{-1} with 10-fold dilution are applied to each subarray and incubated for 1 h at 37 °C. The diluent 0.01 M PBS containing 10% human serum (v/v) is utilized as negative control. After incubation with recognition antibody and Cy3-labeled secondary antibody, all slides are thoroughly washed and then scanned by a scanner LuxScan 10K. Fluorescence images of each subarray on the same slide are shown in Figure 6a, indicating that signal intensity is
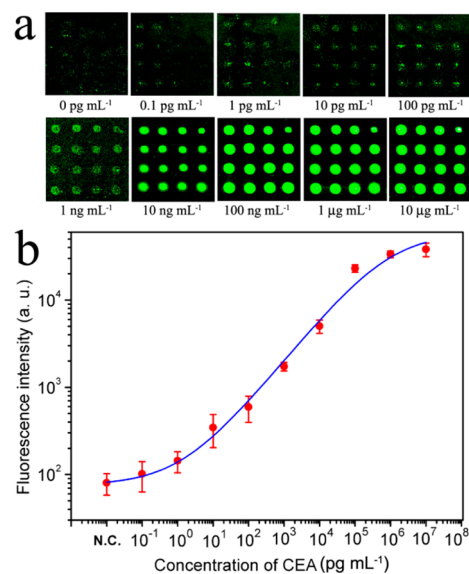

Figure 6. Fluorescence images (a) and dose-dependent curve (b) of microarray for CEA detection in 10% human serum.

increased with an increase of CEA concentration. After quantitatively analyzing, a typical sigmoid dose-dependent curve is plotted with double logarithmic axes (Figure 6b). It can be found that the dynamic range covers 6 orders from 1 pg mL^{-1} to 1 μg mL^{-1}, and LOD is determined to be 1 pg mL^{-1} by 3 standard deviations above the background.[2] The strong fluorescent signal and good dose-dependent response in Figure 6 clearly demonstrate that the adhesion of ZnO NMBs on glass slide is strong enough to survive multistep washing during the assay. Such a high performance in terms of low LOD and wide dynamic range is attributed to ZnO NMB-enabled intrinsic fluorescence enhancement and high protein loading capacity as

discussed above. Furthermore, the analyte could easily access capture antibody immobilized on ZnO NMB because of its 3D structure and large surface area, thus improving antibody–antigen binding efficiency.

In comparison to existing nanostructured substrates,[15,18] ZnO NMB slide renders much lower LOD and broader dynamic range for microarray immunoassay. Besides that, ZnO NMBs coated substrate can be simply fabricated by drop-coating without using any expensive equipment and techniques, providing simple, inexpensive, and mass producible microarray support. It is worthy of a note that ZnO NMB has a variety of merits including very low autofluorescence, good versatility for fluorescence enhancement regardless of fluorescence characteristics, and excellent compatibility with commercially available robotic chipwriter. Moreover, the performance obtained from ZnO NMB slide is even better than or very comparable with that achieved by enzymatic catalysis,[8,9] rolling circle amplification (RCA),[10,36] and scanometric assay.[4,37] Unlike these signal amplification methods, fluorescence signal can be directly enhanced by ZnO NMB without any downstream biochemical or chemical reactions required, leading to simple, low cost, and accurate detections. Thus, the advanced ZnO NMBs coated substrate provides a great potential to simultaneously screen large numbers of proteins on microarray platform with high sensitivity even in complex biological fluid such as serum. Such a capability in terms of high-throughput and high sensitivity is very critical for parallel screening of multiple biomarkers and large number of samples in early diagnosis.

4. CONCLUSIONS

In summary, ZnO NMB with low autofluorescence and significant fluorescence amplification capability is demonstrated for the first time as a superior coating material for sensitive microarray immunoassay. A low detection limit (1 pg mL^{-1}) and a wide dynamic range (1 pg mL^{-1} to 1 μg mL^{-1}) are successfully achieved on ZnO NMB coated glass slide with a cancer biomarker CEA as a model analyte. Results further reveal that the significant signal enhancement is attributed to ZnO-resulting intrinsic fluorescence amplification and high protein loading capacity. The developed substrate has prominent advantages including facile mass fabrication, low autofluorescence, versatility for various fluorophores, and good compatibility with existing robotic microarrayer, thus providing a great promise for economic, sensitive, and high-throughput disease biomarker screening in early diagnosis.

■ AUTHOR INFORMATION

Corresponding Author
*Phone: +86-23-68254727. Fax: +86-23-68254969. E-mail: ecmli@swu.edu.cn.

Notes
The authors declare no competing financial interest.

■ ACKNOWLEDGMENTS

■ REFERENCES

(1) Liu, Y. S.; Hu, W. H.; Lu, Z. S.; Li, C. M. Photografted Poly(methyl methacrylate)-Based High Performance Protein Microarray for Hepatitis B Virus Biomarker Detection in Human Serum. *MedChemComm* **2010**, *1*, 132−135.

(2) Yu, L.; Liu, Y. S.; Gan, Y.; Li, C. M. High-Performance UV-Curable Epoxy Resin-Based Microarray and Microfluidic Immunoassay Devices. *Biosens. Bioelectron.* **2009**, *24*, 2997−3002.

(3) Cretich, M.; Carlo, G.; Longhi, R.; Gotti, C.; Spinella, N.; Coffa, S.; Galati, C.; Renna, L.; Chiari, M. High Sensitivity Protein Assays on Microarray Silicon Slides. *Anal. Chem.* **2009**, *81*, 5197−5203.

(4) Kim, D. W.; Daniel, W. L.; Mirkin, C. A. A Microarray-Based Multiplexed Scanometric Immunoassay for Protein Cancer Markers Using Gold Nanoparticle Probes. *Anal. Chem.* **2009**, *81*, 9183−9187.

(5) Zhu, H.; Stybayeva, G.; Macal, M.; Ramanculov, E.; George, M. D.; Dandekar, S.; Revzin, A. A Microdevice for Multiplexed Detection of T-Cell-Secreted Cytokines. *Lab Chip* **2008**, *8*, 2197−2205.

(6) Park, E. S.; Brown, A. C.; DiFeo, M. A.; Barker, T. H.; Lu, H. Continuously Perfused, Non-Cross-Contaminating Microfluidic Chamber Array for Studying Cellular Responses to Orthogonal Combinations of Matrix and Soluble Signals. *Lab Chip* **2010**, *10*, 571−580.

(7) Diaz-Quijada, G. A.; Peytavi, R.; Nantel, A.; Roy, E.; Bergeron, M. G.; Dumoulin, M. M.; Veres, T. Surface Modification of Thermoplastics—Towards the Plastic Biochip for High Throughput Screening Devices. *Lab Chip* **2007**, *7*, 856−862.

(8) Woodbury, R. L.; Varnum, S. M.; Zangar, R. C. Elevated HGF Levels in Sera from Breast Cancer Patients Detected Using a Protein Microarray ELISA. *J. Proteome Res.* **2002**, *1*, 233−237.

(9) Wolter, A.; Niessner, R.; Seidel, M. Preparation and Characterization of Functional Poly(ethylene glycol) Surfaces for the Use of Antibody Microarrays. *Anal. Chem.* **2007**, *79*, 4529−4537.

(10) Schweitzer, B.; Roberts, S.; Grimwade, B.; Shao, W. P.; Wang, M. J.; Fu, Q.; Shu, Q. P.; Laroche, I.; Zhou, Z. M.; Tchernev, V. T.; Christiansen, J.; Velleca, M.; Kingsmore, S. F. Multiplexed Protein Profiling on Microarrays by Rolling-Circle Amplification. *Nat. Biotechnol.* **2002**, *20*, 359−365.

(11) Nagl, S.; Schaeferling, M.; Wolfbeis, O. S. Fluorescence Analysis in Microarray Technology. *Microchim. Acta* **2005**, *151*, 1−21.

(12) Dorfman, A.; Kumar, N.; Hahm, J. Nanoscale ZnO-Enhanced Fluorescence Detection of Protein Interactions. *Adv. Mater.* **2006**, *18*, 2685−2690.

(13) Bakker, R. M.; Drachev, V. P.; Liu, Z. T.; Yuan, H. K.; Pedersen, R. H.; Boltasseva, A.; Chen, J. J.; Irudayaraj, J.; Kildishev, A. V.; Shalaev, V. M. Nanoantenna Array-Induced Fluorescence Enhancement and Reduced Lifetimes. *New J. Phys.* **2008**, *10*, 125022.

(14) Bakker, R. M.; Yuan, H. K.; Liu, Z. T.; Drachev, V. P.; Kildishev, A. V.; Shalaev, V. M.; Pedersen, R. H.; Gresillon, S.; Boltasseva, A. Enhanced Localized Fluorescence in Plasmonic Nanoantennae. *Appl. Phys. Lett.* **2008**, *92*, 043101.

(15) Mathias, P. C.; Ganesh, N.; Cunningham, B. T. Application of Photonic Crystal Enhanced Fluorescence to a Cytokine Immunoassay. *Anal. Chem.* **2008**, *80*, 9013−9020.

(16) Shankar, S. S.; Rizzello, L.; Cingolani, R.; Rinaldi, R.; Pompa, P. P. Micro/Nanoscale Patterning of Nanostructured Metal Substrates for Plasmonic Applications. *ACS Nano* **2009**, *3*, 893−900.

(17) Moal, E. L.; Leveque-Fort, S.; Potier, M. C.; Fort, E. Nanoroughened Plasmonic Films for Enhanced Biosensing Detection. *Nanotechnology* **2009**, *20*, 225502.

(18) Staiano, M.; Matveeva, E. G.; Rossi, M.; Crescenzo, R.; Gryczynski, Z.; Gryczynski, I.; Iozzino, L.; Akopova, I.; D'Auria, S. Nanostructured Silver-Based Surfaces: New Emergent Methodologies for an Easy Detection of Analytes. *ACS Appl. Mater. Interfaces* **2009**, *1*, 2909−2916.

(19) Im, H.; Lesuffleur, A.; Lindquist, N. C.; Oh, S. H. Plasmonic Nanoholes in a Multi-Channel Microarray Format for Parallel Kinetic Assays and Differential Sensing. *Anal. Chem.* **2009**, *81*, 2854−2859.

(20) Matveeva, E. G.; Gryczynski, I.; Barnett, A.; Leonenko, Z.; Lakowicz, J. R.; Gryczynski, Z. Metal Particle-Enhanced Fluorescent Immunoassays on Metal Mirrors. *Anal. Biochem.* **2007**, *363*, 239−245.

(21) Dorfman, A.; Kumar, N.; Hahm, J. I. Highly Sensitive Biomolecular Fluorescence Detection Using Nanoscale ZnO Platforms. *Langmuir* **2006**, *22*, 4890−4895.

(22) Adalsteinsson, V.; Parajuli, O.; Kepics, S.; Gupta, A.; Reeves, W. B.; Hahm, J. I. Ultrasensitive Detection of Cytokines Enabled by Nanoscale ZnO Arrays. *Anal. Chem.* **2008**, *80*, 6594−6601.

(23) Hu, W. H.; Liu, Y. S.; Zhu, Z. H.; Yang, H. B.; Li, C. M. Randomly Oriented ZnO Nanorods as Advanced Substrate for High-Performance Protein Microarrays. *ACS Appl. Mater. Interfaces* **2010**, *2*, 1569−1572.

(24) Kwok, W. M.; Djurisic, A. B.; Leung, Y. H.; Li, D.; Tam, K. H.; Phillips, D. L.; Chan, W. K. Influence of Annealing on Stimulated Emission in ZnO Nanorods. *Appl. Phys. Lett.* **2006**, *89*, 183112.

(25) Hu, X. L.; Gong, J. M.; Zhang, L. Z.; Yu, J. C. Continuous Size Tuning of Monodisperse ZnO Colloidal Nanocrystal Clusters by a Microwave-Polyol Process and Their Application for Humidity Sensing. *Adv. Mater.* **2008**, *20*, 4845−4850.

(26) Allen, C. G.; Baker, D. J.; Albin, J. M.; Oertli, H. E.; Gillaspie, D. T.; Olson, D. C.; Furtak, T. E.; Collins, R. T. Surface Modification of ZnO Using Triethoxysilane-Based Molecules. *Langmuir* **2008**, *24*, 13393−13398.

(27) Li, C. G.; Zhao, Y.; Wang, L.; Li, G. H.; Shi, Z.; Feng, S. H. Polyol-Mediated Synthesis of Highly Water-Soluble ZnO Colloidal Nanocrystal Clusters. *Eur. J. Inorg. Chem.* **2010**, 217−220.

(28) Carbone, R.; Marni, M. D.; Zanardi, A.; Vinati, S.; Barborini, E.; Fornasari, L.; Milani, P. Characterization of Cluster-Assembled Nanostructured Titanium Oxide Coatings as Substrates for Protein Arrays. *Anal. Biochem.* **2009**, *394*, 7−12.

(29) Hu, W. H.; Li, C. M.; Dong, H. Poly(pyrrole-*co*-pyrrole propylic acid) Film and Its Application in Label-Free Surface Plasmon Resonance Immunosensors. *Anal. Chim. Acta* **2008**, *630*, 67−74.

(30) Liu, Y. S.; Li, C. M.; Yu, L.; Chen, P. Optimization of Printing Buffer for Protein Microarrays Based on Aldehyde-Modified Glass Slides. *Front. Biosci.* **2007**, *12*, 3768−3773.

(31) Liu, Y. S.; Li, C. M.; Hu, W. H.; Lu, Z. S. High Performance Protein Microarrays Based on Glycidyl Methacrylate-Modified Polyethylene Terephthalate Plastic Substrate. *Talanta* **2009**, *77*, 1165−1171.

(32) Hu, W. H.; Lu, Z. S.; Liu, Y. S.; Li, C. M. In Situ Surface Plasmon Resonance Investigation of the Assembly Process of Multiwalled Carbon Nanotubes on an Alkanethiol Self-Assembled Monolayer for Efficient Protein Immobilization and Detection. *Langmuir* **2010**, *26*, 8386−8391.

(33) Yu, L.; Li, C. M.; Liu, Y. S.; Gao, J.; Wang, W.; Gan, Y. Flow-Through Functionalized PDMS Microfluidic Channels with Dextran Derivative for ELISAs. *Lab Chip* **2009**, *9*, 1243−1247.

(34) Nijdam, A. J.; Zianni, M. R.; Herderick, E. E.; Cheng, M. M. C.; Prosperi, J. R.; Robertson, F. A.; Petricoin, E. F.; Liotta, L. A.; Ferrari, M. Application of Physicochemically Modified Silicon Substrates as Reverse-Phase Protein Microarrays. *J. Proteome Res.* **2009**, *8*, 1247−1254.

(35) Gutmann, O.; Kuehlewein, R.; Reinbold, S.; Niekrawietz, R.; Steinert, C. P.; Heij, B. D.; Zengerle, R.; Daub, M. Fast and Reliable Protein Microarray Production by a New Drop-in-Drop Technique. *Lab Chip* **2005**, *5*, 675−681.

(36) Ou, L. J.; Liu, S. J.; Chu, X.; Shen, G. L.; Yu, R. Q. DNA Encapsulating Liposome Based Rolling Circle Amplification Immunoassay as a Versatile Platform for Ultrasensitive Detection of Protein. *Anal. Chem.* **2009**, *81*, 9664−9673.

(37) Wang, Z. X.; Lee, J.; Cossins, A. R.; Brust, M. Microarray-Based Detection of Protein Binding and Functionality by Gold Nanoparticle Probes. *Anal. Chem.* **2005**, *77*, 5770−5774.